Rare Metal Materials and Engineering
Volume 47, Suppl. 2, August 2018
Cite this article as: Rare Metal Materials and Engineering, 2018, 47(S2): 167-170.

PVP Assisted Hydrothermal Synthesis of Bi_2WO_6 Nanoflowers and Their Photocatalytic Activity

Li Wenqi[1], Ding Xingeng[1], Ren Chunrong[1], Wu Huating[1], Yang Hui[1,2]

[1] Zhejiang University, Hangzhou 310027, China; [2] Zhejiang-California International NanoSystems Institute, Hangzhou 310058, China

Abstract: Hollow Bi_2WO_6 nanoflowers were synthesized by a PVP modified hydrothermal method, and their morphology and structure were characterized by XRD, SEM, TEM, PL and UV-vis analysis. A series of controlling experiments indicate PVP plays an important role in the formation of the hollow hierarchical structure. Without adding PVP, the morphology of Bi_2WO_6 is the solid nanoplate. When a small amount of PVP is added, the surface of Bi_2WO_6 splits, and the hollow flowerlike morphology forms. The crystalline size of Bi_2WO_6 also slightly increases with PVP content increasing. The as-prepared PVP-Bi_2WO_6 shows the improved photocatalytic activity under visible light irradiation. PL spectra show that the emission intensity of PVP assisted Bi_2WO_6 is weaker than that of pure PVP, which means the high-mobility of PVP-Bi_2WO_6 is obtained. PVP assisted Bi_2WO_6 nanoflower can be potentially used for practical waste water treatments.

Key words: bismuth tungstate; PVP; photocatalytic activity; hydrothermal method

Contamination of organic pollutants in water has brought a challenge to sustainable environment and human health[1–3]. Visible-light-induced photocatalysts, such as Bi_2WO_6, Ag_3PO_4, WO_3 and g-C_3N_4, have attracted much attention for their good photodegradation efficiency and no secondary environmental pollution[4–8]. Among these visible light photocatalysts, Bi_2WO_6 photocatalyst possesses the small bandgap and excellent chemical stability, which is of benefit for pollutant adsorption and degradation. Generally, the photocatalytic activity is mainly dependent on the morphology and structure. Recently, 3D spherical superstructures have been achieved much attention due to the easier retrievability, the larger surface area, the better physical and chemical properties. This self- assembled structure promotes carrier migration and dye adsorption, which is always designed to be used in photocatalytic fields.

Bi_2WO_6, as one of the simplest member of the Aurivillius family, is constructed by alternating $(Bi_2O_2)_n^{2n+}$ layers and perovskite-like $(WO_4)_n^{2n-}$ layers[9]. Zhang et al. prepared flower-like Bi_2WO_6 superstructures constructed by oriented nanoplates via a simple template-free hydrothermal method[10]. Wu et al. synthesized Bi_2WO_6 hollow nanospheres in water-ethanol mixed solvent using Bi as sacrificial templates[11]. Xu et al. used EDTA as the surfactant to fabricate the nest-like Bi_2WO_6[12]. This self- assembled hollow structure exhibits excellent adsorption ability and carrier mobility, which needs further study and design.

Hence, hollow Bi_2WO_6 nanostructures were synthesized by a PVP modified hydrothermal method, and their morphology and structure were characterized by SEM, TEM, XRD, PL, and UV-vis analysis. Moreover, the photodegradation of RhB was employed to evaluate the photocatalytic activity of as-prepared samples. The relationship between morphology and photocatalytic activity was discussed too.

1 Experiment

Bi_2WO_6 nanoflowers were synthesized through a simple hydrothermal method. Typically, 0.979 g $Bi(NO_3)_3$ $5H_2O$ was dissolved into 40 mL mixture solutions, which contained 8 mL glacial acetic acid, 8 mL ethanol and 24 mL deionized water (marked as A). At the same time, 0.331 g Na_2WO_4 $2H_2O$ was dissolved into 30 mL deionized water (marked as B). After stirring for 30 min, 0, 0.05, 0.1 and 0.2 g PVP were added into the A separately. Finally, solution B was added into the solution dropwise, and transferred into a 100 mL Teflon-lined autoclave. The autoclave was sealed and heated to 140 ℃ for 12 h. Finally, the products were collected from the solution by centrifugation and sequentially washed with deionized water and ethanol for several times, and dried at 60 ℃ for 12 h.

The products were characterized by X-ray powder diffraction using a diffractometer with Cu Kα wavelength ($\lambda_{K\alpha1}$=0.154 060 nm and $\lambda_{K\alpha2}$=0.154 443 nm). The cell parameters of Bi_2WO_6 nanoflowers were calculated by (113) diffraction peak. For this

Received date: August 25, 2017
Foundation item: The National High-Tech Research and Development Program of China (“863” Program) (2015AA034701)
Corresponding author: Ding Xingeng, Ph. D., Associate Professor, School of Materials Science and Engineering, Zhejiang University, Hangzhou 310027, P. R. China, Tel: 0086-571-87952408, E-mail: msedxg@zju.edu.cn

purpose, data were collected over the angle arrange 20°~80° with a step size of 0.02°. The morphology and microstructure of the samples were measured by scanning electron microscopy (FESEM, SU-70). High resolution transmission electron microscopy (HRTEM) were obtained using a Tecnai G2 F20 S-TWIN FEI transmission electron microscope operated at 200 kV. The photoluminescence (PL) spectra were recorded with an F-4500 fluorescence spectrophotometer.

The photocatalytic activity of the Bi_2WO_6 nanoflowers was investigated by the photodegradation of Rhodamine B (RhB, 10 mg/L). In the typical experiment, 30 mg Bi_2WO_6 powders were ground uniformly, and then added into the 100 mL RhB solution. Subsequently, suspensions were magnetically stirred in the dark for 30 min to establish adsorption-desorption equilibrium. At each 30 min interval, 5 mL solution was collected and then centrifuged to obtain supernatant liquid. The concentration of RhB was determined at 554 nm by a UV-vis spectrophotometer (UV-3150).

The photodegradation rate of RhB was calculated by the following equation:

$$D_{(RhB)}=1-C_t/C_0 \quad (1)$$

where C_0 is the initial concentration of RhB, and the C_t is the concentration of RhB after light radiation for t min[13].

2 Result and Discussion

2.1 Microstructure and morphology of the as-prepared samples

Fig.1 shows the XRD patterns of PVP-Bi_2WO_6 nanoflowers. All the diffraction peaks of samples can be indexed to be the pure orthorhombic phase of Bi_2WO_6 (JCPDS card no. 39-0256). No other peaks of impurities are found, indicating high purity of samples. The results show that the intensity of samples decreases to a minimum value and then increases with the increase of PVP content. Similarly, the smallest crystalline size of samples is 13.4 nm when the PVP content is 0.05 g (Table 1). The crystalline size is closely related to specific surface area, which mainly affects the adsorption of dye.

Fig.2 displays the SEM images of as-prepared samples. Without adding PVP, the morphology of Bi_2WO_6 mainly consists of larger nanoplates, and some small and thin pieces grow on the plates. When 0.05 g PVP is added, the quantity of small plates increases, which are connected to each other to form the uniform microspheres. The flower-like microspheres are 3~4 μm in diameter and are made up of nanosheets. The gaps between neighbor nanosheets are observed in the range

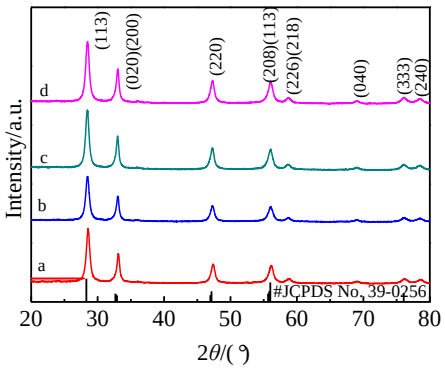

Fig.1 XRD patterns of Bi_2WO_6 nanoflowers with adding different amount of PVP: (a) 0, (b) 0.05 g, (c) 0.1 g, and (d) 0.2 g

Table 1 Lattice parameter of PVP assisted Bi_2WO_6 nanoflowers[9]

	2θ	a/nm	FWHM	Crystalline size/nm
a	28.535	0.540 70	0.614	13.6
b	28.449	0.542 07	0.611	13.4
c	28.413	0.542 51	0.551	15.1
d	28.490	0.541 75	0.494	17.0

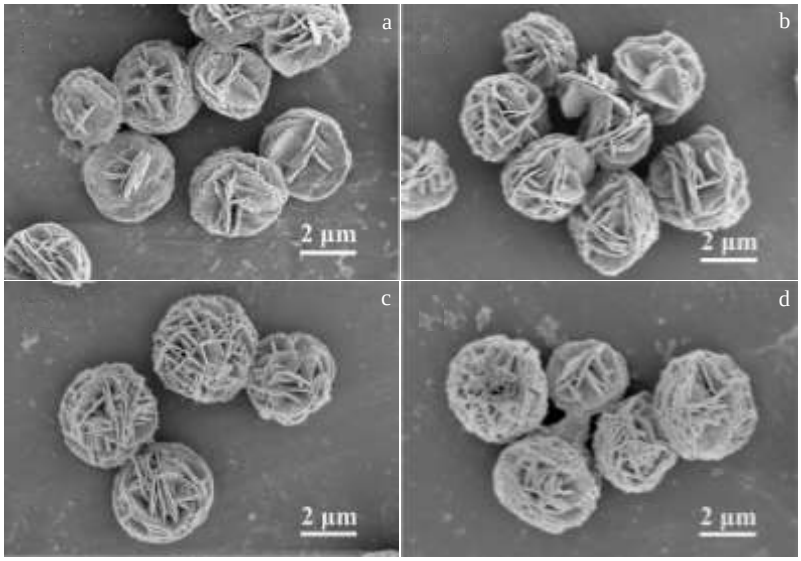

Fig.2 SEM images of Bi_2WO_6 nanoflowers with adding different amounts of PVP: (a) 0, (b) 0.05 g, (c) 0.1 g, and (d) 0.2 g

from several dozens to several hundred nanometers. With the PVP content increasing to 0.2 g, the products present dense flower-like morphology (Fig.2c). Based on above analysis, the possible growth mechanism can be described. Orthorhombic Bi_2WO_6 nuclei are firstly formed in the solution, which are constructed by alternating $(Bi_2O_2)_n^{2n+}$ layers and perovskite-like $(WO_4)_n^{2n-}$ layers. These nanoplates are parallel to the (001) facets due to the high chemical potential of (100) and (010) facets. When the PVP is added into the solution, these residual nuclei are spontaneously selected to adsorb on the (001) facets. A small amount of Bi^{3+} ions will be caught by the functional group of the terminal PVP molecules. As a result, small nanoplates are grown perpendicular to the (001) faces, and the flower-like structure forms (Fig.2b). With the increase of PVP concentration, the quantity of vertical nanoplates increases. Finally, the Bi_2WO_6 gradually grows into the spherical nanoflowers.

TEM observation were further carried out to investigate the morphology and structure of 0.2PVP-Bi_2WO_6. As shown in Fig.3a, the sample exhibits the hollow sphere-like structure copping with the nanosheets. The clear lattice fringes with a typical spacing of 0.313 nm can be assigned to (113) lattice planes of Bi_2WO_6. Based on the XRD analysis, the microspheres are identified as orthorhombic Bi_2WO_6.

2.2 Photocatalytic tests

The photocatalytic activity of as-prepared samples was investigated by the degradation of RhB. To ensure the adsorption-desorption balance is achieved between the catalyst and dye, the 100 mL RhB solution contained with 30 mg PVP-Bi_2WO_6 powder is stirred for 30 min in the dark. The photodegradation of RhB under visible light (λ>420 nm) is shown in Fig.4a. It can be noted that introducing PVP in Bi_2WO_6 nanoflowers can effectively improve the photocatalytic degradation rate. Under 3 h visible light irradiation, the corresponding RhB degradation degree of Bi_2WO_6, 0.05PVP-Bi_2WO_6, 0.1PVP-Bi_2WO_6, 0.2PVP-Bi_2WO_6 is 20%, 31%, 32% and 46%, respectively. Meanwhile, a pseudo-first-order kinetic model was carried out to fit the degradation of RhB. The kinetic of Bi_2WO_6 and 0.2PVP-Bi_2WO_6 is 0.00130 and 0.0034 min^{-1}, respectively.

PL spectra are usually used to investigate the mitigation, transfer and recombination electron-hole pairs. Generally, the low intensity of excitation peaks indicates the low recombination of electron-hole pairs[14]. As shown in Fig.5, all the samples show emission band centered at around 370~410 nm. The over-all emission intensity of PVP-Bi_2WO_6 is obviously reduced compared with that of pure Bi_2WO_6, which means

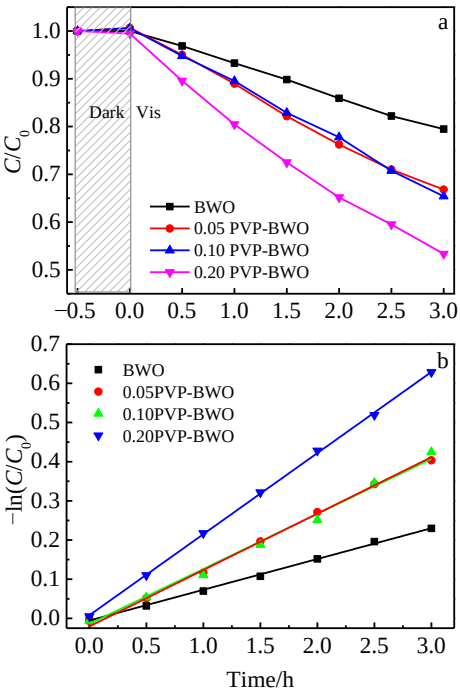

Fig.4 Photocatalytic degradation of RhB in the presence of PVP-Bi_2WO_6 nanoflowers under visible light irradiation (a); the corresponding kinetic fit for the degradation of RhB with PVP-Bi_2WO_6 nanoflower (b)

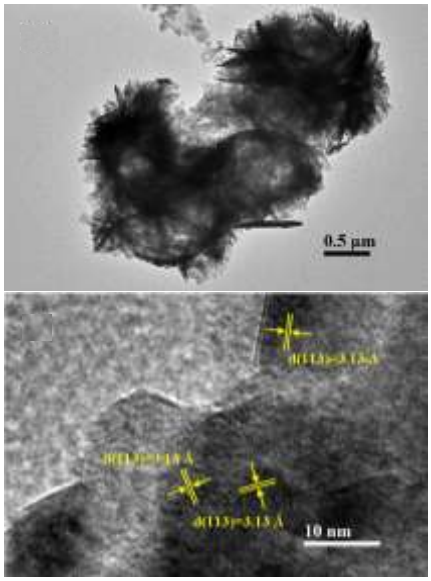

Fig.3 TEM images of 0.2PVP-Bi_2WO_6 nanoflowers

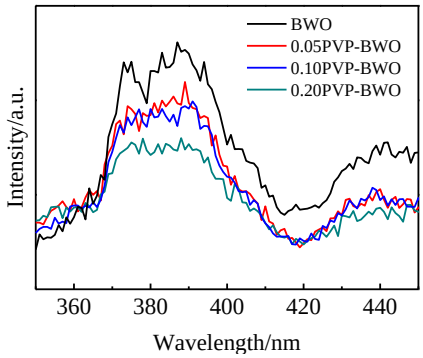

Fig.5 Fluorescence spectra (PL) of PVP-Bi_2WO_6 nanoflowers

introducing PVP into Bi_2WO_6 can effectively facilitate the carrier separation. In addition, the PL peak of 0.2PVP-Bi_2WO_6 composite shows the lowest intensity.

Finally, the mechanism of improved photocatalytic activity of PVP-Bi_2WO_6 was discussed. An effective photocatalytic reaction needs good adsorption ability and photocatalytic activity. The standard redox potential of Bi^{V}/Bi^{III} is more negative than that of OH^-/H_2O, which means the hole generated on the surface of Bi_2WO_6 cannot react with OH^-/H_2O to form OH. The reactions can be described by the following equations. Organic pollutants first is adsorbed on the surface of Bi_2WO_6, and then directly react with photogenerated holes (h^+). Based on analysis of its crystal structure and morphology, the PVP assisted Bi_2WO_6 provides a 3D-porous nanoflowers structure, which has high specific surface area and good carrier separation ability. Li et al. found PVP could be adsorbed on the surface of samples by a strong donor-acceptor interaction via C=O bonds[15]. It leads to an enhanced zeta potential and stronger adsorption capacity, which makes RhB molecules much easier to be adsorbed on the surface of Bi_2WO_6. In conclusion, PVP-Bi_2WO_6 nanoflowers exhibit good adsorption ability and photocatalytic activity, which can be potentially used in practical applications.

$$Bi_2WO_6 + h\nu \rightarrow h^+ + e^- \quad (2)$$

$$h^+ + dye \rightarrow CO_2 + H_2O + \cdots \quad (3)$$

3 Conclusions

1) Hollow Bi_2WO_6 nanostructures have been successfully synthesized by the PVP modified hydrothermal method.

2) With the assistance of PVP, the Bi_2WO_6 is preferential assembled to the hollow flower-like structure. PVP molecules are adsorbed on the (100) facets and capture Bi^{3+} and WO_4^{2-} ions to form the small nanoplates.

3) The PVP assisted Bi_2WO_6 shows the high specific surface area and the mesoporous structure, which facilitates transfer and separation of carriers.

4) 0.2 g PVP assisted Bi_2WO_6 exhibits high photocatalytic activity, and the pseudo-first-order kinetic is 0.00130 min^{-1}. PVP assisted Bi_2WO_6 nanoflowers could be regarded as a potential candidate for practical waste water treatments.

References

1 Tian J, Sang Y, Yu G *et al. Advanced Materials*[J], 2013, 25(36): 5075
2 Sahara G, Ishitani O. *Inorganic Chemistry*[J], 2015, 54(11): 5096
3 Kudo A, Miseki Y. *Chemical Society Reviews*[J], 2008, 38: 253
4 Zhang N, Ciriminna R, Pagliaro M *et al*. *Chemical Society Reviews*[J], 2014, 43(15): 5276
5 Chen X, Shen S, Guo L *et al*. *Chemical Reviews*[J], 2010, 110(11): 6503
6 Di J, Xia J, Ge Y *et al*. *Applied Catalysis B Environmental*[J], 2015, s168-169: 51
7 Zhou Y, Tian Z, Zhao Z *et al*. *ACS Appl Mater Interfaces*[J], 2011, 3(9): 3594
8 Li C, Chen G, Sun J *et al*. *Applied Catalysis B Environmental*[J], 2015, 163: 415
9 Zhang L, Wang H, Chen Z *et al*. *Applied Catalysis B Environmental*[J], 2011, 106(1-2): 1
10 Zhang L, Wang W, Chen Z *et al*. *Journal of Materials Chemistry*[J], 2007, 17(24): 2526
11 Wu D, Zhu H, Zhang C *et al*. *Chemical Communications*[J], 2010, 46(38): 7250
12 Xu L, Yang X, Zhai Z *et al*. *Crystengcomm*[J], 2011, 13(24): 7267
13 Di J, Xia J, Ge Y *et al*. *Applied Catalysis B Environmental*[J], 2015, s168-169: 51
14 Tian Y, Hua G, Xu W *et al*. *Journal of Alloys and Compounds*[J], 2011, 509(3): 724
15 Li Y, Wang Z, Huang B *et al*. *Applied Surface Science*[J], 2015, 347: 258

PVP 辅助水热合成 Bi_2WO_6 纳米花及其光催化活性

李文琪[1]，丁新更[1]，任春溶[1]，巫华婷[1]，杨　辉[1,2]

(1. 浙江大学，浙江 杭州 310027)

(2. 浙江加州国际纳米技术研究院，浙江 杭州 310058)

摘　要：本实验成功利用 PVP（聚乙烯吡咯烷酮）辅助水热技术合成了 Bi_2WO_6 空心纳米花，并对其结构和形貌进行了 X 射线衍射、扫描电子显微镜、透射电子显微镜、荧光光谱和紫外可见漫反射谱表征。结果表明：PVP 对 Bi_2WO_6 空心纳米花的形成起到关键作用。在未添加 PVP 时，钨酸铋呈现出实心的纳米片状堆叠的结构，仅在纳米片的表面垂直生长少量小片。而随着 PVP 的量增多，表面的钨酸铋纳米片发生劈裂，垂直生长的纳米片数量增多，以至最终形成了空心的纳米花状结构。同时，钨酸铋的晶粒尺寸随着 PVP 含量的增加呈现出先减小再增大的趋势。基于 PVP 对其比表面积和吸附能力的改善，这种空心的钨酸铋纳米花展现出良好的光催化性能。在 35W 金卤灯模拟的可见光照射下，3 h 内对罗丹明 B 的降解率达到了 47%。荧光光谱分析表明 PVP 辅助水热的钨酸铋纳米花也具有更高的载流子迁移率。

关键词：钨酸铋；PVP；光催化活性；水热法

作者简介：李文琪，男，1989 年生，博士生，浙江大学材料科学与工程学院，浙江 杭州 310027，电话：0571-8795408，E-mail: liwq@zju.edu.cn